

## Exploring Thermally Radiant Williamson Nanofluid Analysis on an Exponentially Stretching Sheet with Chemical Reaction via the Homotopy Analysis Method.

K saikumar, Department of ECE, Koneru Lakshmaiah Education Foundation, India-522302,

[saikumarkayam4@ieee.org](mailto:saikumarkayam4@ieee.org)

SK ahammad , Department of ECE, Koneru Lakshmaiah Education Foundation, India-522302,

### Abstract

This paper investigates the impact of thermal radiation, viscous dissipation, and chemical reaction on the stagnation point flow of Williamson nanofluid over an exponentially stretching sheet. The study utilizes similarity transformations to convert partial differential equations (PDEs) into ordinary differential equations (ODEs), and the simulation is carried out using the homotopy analysis method (HAM). Comparisons with existing literature validate the accuracy of our findings for specific scenarios. Graphs and tables are presented to illustrate the behavior of skin friction, Nusselt number, and Sherwood numbers for various values of flow parameters. Notably, the skin friction coefficient exhibits enhancement with an increase in the Williamson fluid parameter.

### Introduction

Nanofluids, consisting of nanometer-sized particles below 100 nanometres, are introduced into various base fluids like oil, water, bio fluids, ethylene, and lubricants. These nanofluids have gained significant attention from researchers due to their immense potential in industries, medicine, and various scientific and technological domains. Their unique properties make them stand out from conventional fluids [1]-[2].

Despite the extensive research on nanofluids, they remain indispensable in specific areas, especially in the medical sector. For instance, gold nanoparticles are used for cancerous tumor screening and the development of tiny bombs for cancer eradication [3]. The concept of using nanomaterials in fluids to enhance thermal conductivity was first introduced [4-6]. They observed that the infusion of nanoparticles into fluids strengthened their thermal conductivity. [7] have produced analytical solutions for the behavior of magnetohydrodynamic (MHD) nanofluids in squeezing flow between two parallel plates. [8-10] investigated the distribution of heat and mass over a radially stretched surface using electrically conducting nanofluids, considering thermophoresis and Brownian motion. Additionally, [11-13] explored the impact of increasing nonlinear thermal radiation on boundary layer flow of various nanofluids. Overall, nanofluids continue to captivate the scientific community due to their

potential and diverse applications, making them a promising area of research in the field of fluid dynamics and nanotechnology [14].

## Mathematical formulation

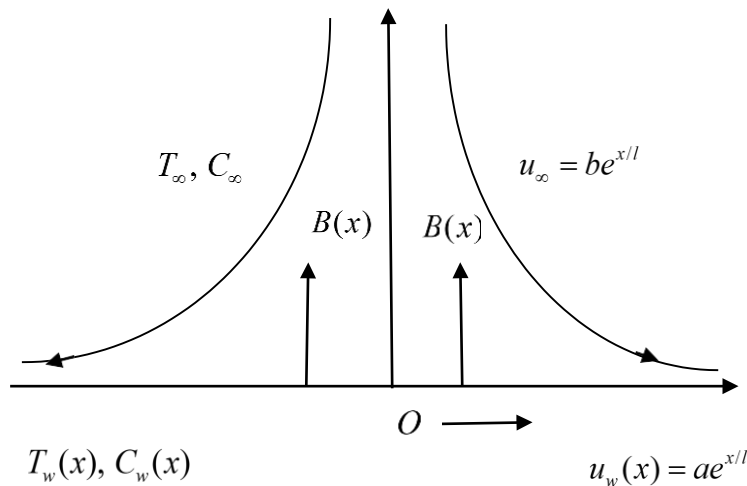


Figure 1 Physical model of the flow

The governing boundary layer equations

$$\frac{\partial u}{\partial x} + \frac{\partial v}{\partial y} = 0, \quad (1)$$

$$u \frac{\partial u}{\partial x} + v \frac{\partial u}{\partial y} = \sqrt{2\nu} \Gamma \frac{\partial u}{\partial y} \frac{\partial^2 u}{\partial y^2} + u_\infty \frac{du_\infty}{dx} + \nu \frac{\partial^2 u}{\partial y^2} + \frac{\sigma B^2(x)}{\rho_f} [u_\infty - u], \quad (2)$$

$$u \frac{\partial T}{\partial x} + v \frac{\partial T}{\partial y} = \alpha \frac{\partial^2 T}{\partial y^2} - \frac{1}{(\rho C_p)_f} \frac{\partial q_r}{\partial y} + \tau \left[ D_B \left( \frac{\partial C}{\partial y} \frac{\partial T}{\partial y} \right) + \frac{D_T}{T_\infty} \left( \frac{\partial T}{\partial y} \right)^2 \right] + \frac{\mu}{(\rho C_p)_f} \left( \frac{\partial u}{\partial y} \right)^2, \quad (3)$$

$$u \frac{\partial C}{\partial x} + v \frac{\partial C}{\partial y} = D_B \left( \frac{\partial^2 C}{\partial y^2} \right) + \frac{D_T}{T_\infty} \left( \frac{\partial^2 T}{\partial y^2} \right) - Kr(C - C_\infty). \quad (4)$$

Subject to the boundary conditions

$$\begin{aligned} u = u_w(x) = ae^{x/l}, \quad v = 0, \quad T = T_w(x), \quad C = C_w(x) \quad \text{at } y = 0 \\ u \rightarrow u_\infty(x) = be^{x/l}, \quad v \rightarrow 0, \quad T \rightarrow T_\infty, \quad C \rightarrow C_\infty \quad \text{as } y \rightarrow \infty \end{aligned} \quad (5)$$

The following similarity transformations are now introduced:

$$\psi = \sqrt{2lva} e^{x/2l} f(\zeta), \theta(\zeta) = \frac{T - T_\infty}{T_w - T_\infty}, \phi(\zeta) = \frac{C - C_\infty}{C_w - C_\infty}, \zeta = y\sqrt{a/2vl}e^{x/2l}. \quad (6)$$

Now Eq. (2) to Eq. (5) become

$$f''' + \lambda f'' f''' + ff'' - 2f'^2 + 2\varepsilon^2 + M(\varepsilon - f') = 0, \quad (7)$$

$$\frac{1}{Pr} \left( 1 + \frac{4R}{3} \right) \theta'' + f\theta' - f'\theta + Nb\phi'\theta' + Nt\theta'^2 + Ec f'^2 = 0, \quad (8)$$

$$\phi'' + Le f\phi' - Le f'\phi + \frac{Nt}{Nb} \theta'' - \gamma Le\phi = 0. \quad (9)$$

The boundary conditions are

$$\begin{aligned} f(\zeta) = 0, f'(\zeta) = 1, \theta(\zeta) = 1, \phi(\zeta) = 1 \quad \text{at } \zeta = 0, \\ f'(\zeta) \rightarrow \varepsilon, \theta(\zeta) \rightarrow 0, \phi(\zeta) \rightarrow 0 \quad \text{as } \zeta \rightarrow \infty. \end{aligned} \quad (10)$$

We practice the mentioned initial guesses and linear operators to summarize the homotopic approaches of Eq. (7) to Eq. (10).

$$(1-p)L_1(f(\zeta; p) - f_0(\zeta)) = p\hbar_1 N_1[f(\zeta; p)], \quad (11)$$

$$(1-p)L_2(\theta(\zeta; p) - \theta_0(\zeta)) = p\hbar_2 N_2[f(\zeta; p), \theta(\zeta; p), \phi(\zeta; p)], \quad (12)$$

$$(1-p)L_3(\phi(\zeta; p) - \phi_0(\zeta)) = p\hbar_3 N_3[f(\zeta; p), \theta(\zeta; p), \phi(\zeta; p)], \quad (13)$$

Subject to the boundary conditions

$$\begin{aligned} f(0; p) &= 0, & f'(0; p) &= 1, & f'(\infty; p) &= \varepsilon, \\ \theta(0; p) &= 1, & & & \theta(\infty; p) &= 0, \\ \phi(0; p) &= 1, & & & \phi(\infty; p) &= 0, \end{aligned} \quad (14)$$

where

$$\begin{aligned} N_1[f(\zeta; p)] &= \frac{\partial^3 f(\zeta; p)}{\partial \zeta^3} + \lambda \frac{\partial^2 f(\zeta; p)}{\partial \zeta^2} \frac{\partial^3 f(\zeta; p)}{\partial \zeta^3} + f(\zeta; p) \frac{\partial^2 f(\zeta; p)}{\partial \zeta^2} \\ &- 2 \left( \frac{\partial f(\zeta; p)}{\partial \zeta} \right)^2 + 2\varepsilon^2 + M \left( \varepsilon - \frac{\partial f(\zeta; p)}{\partial \zeta} \right), \end{aligned} \quad (15)$$

$$\begin{aligned} N_2[f(\zeta; p), \theta(\zeta; p), \phi(\zeta; p)] &= \frac{1}{Pr} \left( 1 + \frac{4}{3} R \right) \frac{\partial^2 \theta(\zeta; p)}{\partial \zeta^2} \\ &+ \left( f(\zeta; p) \frac{\partial \theta(\zeta; p)}{\partial \zeta} - \theta(\zeta; p) \frac{\partial f(\zeta; p)}{\partial \zeta} \right) + Nb \frac{\partial \theta(\zeta; p)}{\partial \zeta} \frac{\partial \phi(\zeta; p)}{\partial \zeta} \\ &+ Nt \left( \frac{\partial \theta(\zeta; p)}{\partial \zeta} \right)^2 + Ec \left( \frac{\partial f(\zeta; p)}{\partial \zeta} \right)^2, \end{aligned} \quad (16)$$

$$\begin{aligned} N_3[f(\zeta; p), \theta(\zeta; p), \phi(\zeta; p)] &= \frac{\partial^2 \phi(\zeta; p)}{\partial \zeta^2} + Le f(\zeta; p) \frac{\partial \phi(\zeta; p)}{\partial \zeta} \\ &- Le \theta(\zeta; p) \frac{\partial f(\zeta; p)}{\partial \zeta} + \frac{Nt}{Nb} \frac{\partial^2 \theta(\zeta; p)}{\partial \zeta^2} - Le \gamma \phi(\zeta; p), \end{aligned} \quad (17)$$

The  $n^{\text{th}}$  order distortion equations are as follows

$$L_1(f_n(\zeta) - \chi_n f_{n-1}(\zeta)) = \hbar_1 R_n^f(\zeta), \quad (18)$$

$$L_2(\theta_n(\zeta) - \chi_n \theta_{n-1}(\zeta)) = \hbar_2 R_n^\theta(\zeta), \quad (19)$$

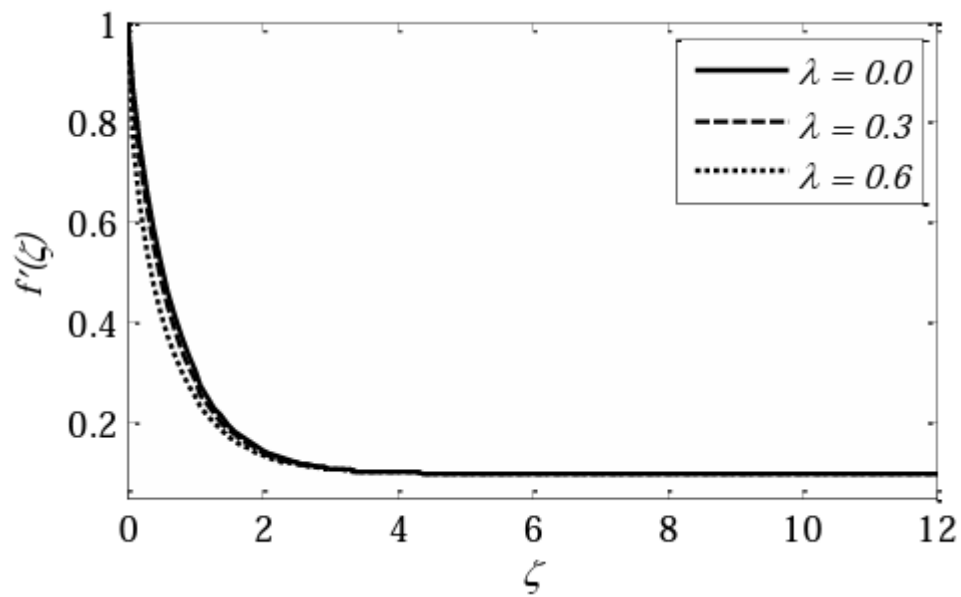
$$L_3(\phi_n(\zeta) - \chi_n \phi_{n-1}(\zeta)) = \hbar_3 R_n^\phi(\zeta), \quad (20)$$

with the following boundary conditions

$$\begin{aligned} f_n(0) &= 0, & f_n'(0) &= 0, & f_n'(\infty) &= 0, \\ \theta_n(0) &= 0, & & & \theta_n(\infty) &= 0, \\ \phi_n(0) &= 0, & & & \phi_n(\infty) &= 0, \end{aligned} \quad (21)$$

## Results

The Homotopy Analysis Method (HAM) has been utilized to solve the modified equations subjected to specific boundary conditions [15]. Graphs representing different profiles are plotted for various values of the controlling parameters.

Figure 2: Profiles of  $f'(\zeta)$  for  $\lambda$

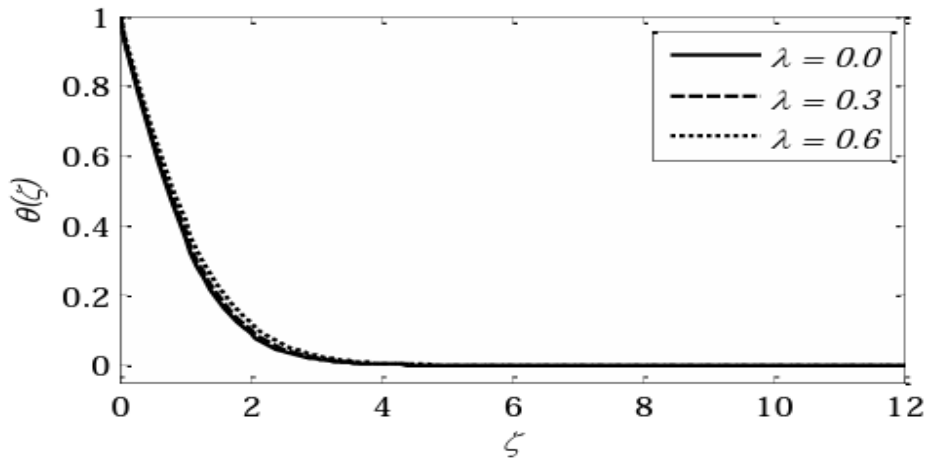


Fig. 4. Profiles of  $\theta(\zeta)$  for  $\lambda$

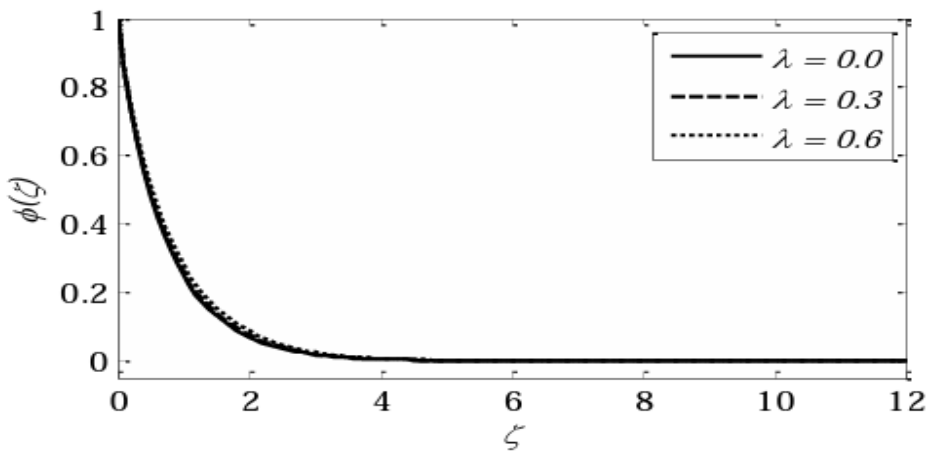


Fig. 5. Profiles of  $\phi(\zeta)$  for  $\lambda$

## Conclusions

As the parameter  $\lambda$  is increased, the fluid velocity decreases, but the Skin friction coefficient increases. On the other hand, when  $\varepsilon$  is increased, the velocity profile rises, while the temperature and concentration profiles decrease. The thermal boundary layer thickness reduces with an increase in the Prandtl number, whereas the radiation parameter has the opposite effect.

## References

- [1] Choi, S. US, and Jeffrey A. Eastman. Enhancing thermal conductivity of fluids with nanoparticles. No. ANL/MSD/CP 84938; CONF-951135-29. Argonne National Lab. (ANL), Argonne, IL (United States), 1995.
- [2] Hayat, Tasawar, Rai Sajjad, Ahmed Alsaedi, Taseer Muhammad, and Rahmat Ellahi. "On squeezed flow of couple stress nanofluid between two parallel plates." Results in Physics 7 (2017): 553-561.

- [3] Makinde, Oluwole D., and A. Aziz. "Boundary layer flow of a nanofluid past a stretching sheet with a convective boundary condition." *International Journal of Thermal Sciences* 50, no. 7 (2011): 1326-1332.
- [4] Mahanthesh, B., B. J. Gireesha, and I. L. Animasaun. "Exploration of non-linear thermal radiation and suspended nanoparticles effects on mixed convection boundary layer flow of nanoliquids on a melting vertical surface." *Journal of Nanofluids* 7, no. 5 (2018): 833-843.
- [5] Bhatti, M. M., M. Ali Abbas, and M. M. Rashidi. "Analytic study of drug delivery in peristaltically induced motion of non-Newtonian nanofluid." *Journal of Nanofluids* 5, no. 6 (2016): 920-927.
- [6] Gul, Taza, Saleem Nasir, Saeed Islam, Zahir Shah, and M. Altaf Khan. "Effective Prandtl Number Model Influences on the  $\gamma\text{Al}_2\text{O}_3\text{-H}_2\text{O}$  and  $\gamma\text{Al}_2\text{O}_3\text{-C}_2\text{H}_6\text{O}_2$  Nanofluids Spray Along a Stretching Cylinder." *Arabian Journal for Science & Engineering (Springer Science & Business Media BV)* 44, no. 2 (2019).
- [7] Ibrahim, S. M., G. Lorenzini, P. Vijaya Kumar, and C. S. K. Raju. "Influence of chemical reaction and heat source on dissipative MHD mixed convection flow of a Casson nanofluid over a nonlinear permeable stretching sheet." *International Journal of Heat and Mass Transfer* 111 (2017): 346-355.
- [8] Kumar, Prathi Vijaya, S. Mohammed Ibrahim, and Giulio Lorenzini. "Thermal Radiation and Heat Source Effects on MHD Non-Newtonian Fluid Flow over a Slandering Stretching Sheet with Cross-Diffusion." In *Defect and Diffusion Forum*, vol. 388, pp. 28-38. Trans Tech Publications Ltd, 2018.
- [9] Hayat, T., S. A. Shehzad, and A. Alsaedi. "Soret and Dufour effects on magnetohydrodynamic (MHD) flow of Casson fluid." *Applied Mathematics and Mechanics* 33, no. 10 (2012): 1301-1312.
- [10] Liao, Shijun. *Beyond Perturbation: Introduction to the Homotopy Analysis Method*. CRC Press, 2011.
- [11] Ibrahim, S. M., P. V. Kumar, G. Lorenzini, and E. Lorenzini. "Influence of Joule heating and heat source on radiative MHD flow over a stretching porous sheet with power-law heat flux." *Journal of Engineering Thermophysics* 28, no. 3 (2019): 332-344.
- [12] Hamrelaine, Salim, Fateh Mebarek-Oudina, and Mohamed Rafik Sari. "Analysis of MHD Jeffery Hamel flow with suction/injection by homotopy analysis method." *Journal of Advanced Research in Fluid Mechanics and Thermal Sciences* 58, no. 2 (2019): 173-186.
- [13] Bidin, Biliana, and Roslinda Nazar. "Numerical solution of the boundary layer flow over an exponentially stretching sheet with thermal radiation." *European Journal of Scientific Research* 33, no. 4 (2009): 710-717.

[14] Ishak, Anuar. "MHD boundary layer flow due to an exponentially stretching sheet with radiation effect." *Sains Malaysiana* 40, no. 4 (2011): 391-395.

[15] Raju, K., Pilli, S. K., Kumar, G. S. S., Saikumar, K., & Jagan, B. O. L. (2019). Implementation of natural random forest machine learning methods on multi spectral image compression. *Journal of Critical Reviews*, 6(5), 265-273.